Reaction Kinetics, Mechanisms and Catalysis
https://doi.org/10.1007/s11144-018-1474-1

Stability of titanium-supported layers of potassium titanates in soot oxidation

P. G. Chigrin[1] · E. A. Kirichenko[1] · V. S. Rudnev[2,3] · I. V. Lukiyanchuk[2] · T. P. Yarovaya[2]

Received: 2 July 2018 / Accepted: 15 September 2018

Abstract

The synthesis of catalyst $K_2Ti_2O_5 + K_2Ti_4O_9/TiO_2/TiO_2 + SiO_2/Ti$ for the oxidation of black carbon was carried out. The composition was prepared by the impregnation of an oxidized titanium surface with additionally modified sublayer consisted of anatase nanoparticles by potassium hydroxide. The initial and completion temperature of the catalytic soot afterburning process lays in the range of 340–550 °C and is in good agreement with analogous catalysts used in practice. The applied catalyst layer is resistant to adhesive and cohesive failure. It is characterized by a satisfactory resistance to thermal shock and the action of inhibitors.

Keywords Soot oxidation catalysts · Potassium dititanate · Stability

Introduction

One of the methods of environment protection from incomplete fossil fuel combustion products is the catalytic oxidation of exhaust gases from industrial equipment, including internal combustion engines [1–3]. Nowadays, the most studied and effective catalysts of carbon combustion are cerium-oxide systems: Hf–Ce, La–Ce, Pr–Ce, Fe–Ce, Pt–Ce, Co–Ce, Mn–Ce, Cu–Ce and Sm–Ce [4–14]. Despite a number of the proposed catalyst advantages, their low thermal and mechanical resistance is noted [15]. These disadvantages are partly offset by the catalyst deposition to the layer [16] and/or their stabilization by the inclusion of

✉ P. G. Chigrin
pal_chig@mail.ru

[1] Institute of Materials of Khabarovsk Scientific Centre, Far Eastern Branch of the Russian Academy of Sciences, 153, Tikhookeanskaya Street, Khabarovsk, Russia 680042

[2] Institute of Chemistry, Far Eastern Branch, Russian Academy of Sciences, 159, Prosp. 100-letya Vladivostoka, Vladivostok, Russia 690022

[3] Far Eastern Federal University, 8, Sukhanova Street, Vladivostok, Russia 690950

Published online: 20 September 2018

ZrO_2 to their structure [17]. However, the addition of zirconium dioxide significantly reduces the catalytic activity of the suggested compounds. In addition, an undoubted disadvantage hindering the wide use of oxide-cerium catalysts is their low resistance to the influence of sulfur dioxide and water vapor [18, 19].

According to [6, 20–24], the inclusion of potassium ions to the structure of widely known titanium oxide catalysts (for example, in the form of compounds such as $K_6Ti_4O_{11}$, $K_2Ti_2O_5$, $K_2Ti_4O_9$, $K_2Ti_6O_{13}$) leads to a significant increase in catalytic activity with simultaneous growth of thermal stability. Potassium titanates are promising for application as catalysts for diesel emission afterburning [25–27]. Moreover, potassium titanates catalyze the oxidation of carbon under conditions for both "loose" and "tied" contact and resistant to water vapor and SO_2 [27]. Most studies of potassium titanate catalytic properties are performed on powdered samples. Meanwhile in practice, diesel particulate filters constructions contain the supported catalysts. The activity of such catalysts remains unclear, as well as the influence of catalytic poisons and effect of thermal and mechanical loads on the composition and mechanical resistance of the deposited layers of potassium titanates.

Catalyst carriers and methods for their preparation deserve separate discussion and consideration [28, 29]. Ideally, such carriers should combine high thermal stability and mechanical strength with a sufficiently high surface area and chemical compatibility with catalytically active components. From this point of view, the particular interest is the usage of corrosion-resistant metals as carriers. These carriers should be treated in a special way to produce an intermediate oxide layer with a high adhesion to the metal substrate, whose thickness, chemical composition and porosity can be easily adjusted. Plasma electrolytic oxidation (PEO) method [30–32] is one of the most technologically and environmentally friendly ways of creating oxide layers on the surface of metals and alloys with controlled thickness, composition and surface morphology. The adjustable anodic oxidation of a metal electrode in an electrolyte medium due to the energy of plasma electrical discharges lays in the basis of this method. It is shown that the PEO is a promising method for both the preparation of metal oxide supports of catalytically active compounds and the synthesis of oxide catalysts on metal bases [33–37]. In particular, $CuMoO_4/TiO_2 + SiO_2/Ti$ composites were formed using a combination of PEO and metal extract mixture pyrolysis methods [38]. Carbon black oxidation process begins at temperatures above 270 °C with a maximum burning rate at 410 °C under "loose" contact conditions. The addition of 30–50 nm solvothermal synthesized anatase nanoparticles layer on the PEO coating have a result in a decrease in the size of the copper molybdate particles, an increase in the mechanical stability of the $CuMoO_4/TiO_2/TiO_2 + SiO_2/Ti$ composites and a decrease in the temperature of the maximum burning rate by $\sim$ 50 °C [39].

Thus, the goal of this work is the formation of coating containing potassium titanates on titanium substrate preliminarily treated with PEO method and subsequent addition of solvothermal synthesized anatase nanoparticles and to study their catalytic ability to burn soot, thermal stability, resistance to mechanical loads and inhibitors.

Experimental

Preparation of PEO coatings

The PEO coatings $TiO_2 + SiO_2$/Ti on wire samples of technical titanium VT1-0 (> 99% Ti) were formed in the galvanostatic mode at $i = 0.2$ A/cm^2 for 10 min in a silicate electrolyte containing 0.05 mol/L Na_2SiO_3 and 0.05 mol/L NaOH [32]. The thickness of the formed coatings was $\sim$ 10–12 μm.

Synthesis of potassium titanate coatings

Before the synthesis of potassium titanate coatings, the oxidized titanium was treated with a colloidal suspension previously obtained by hydrothermal synthesis [40] and containing anatase nanoparticles (30–40 nm). The suspension was applied by dipping, and then the surplus was removed by putting the samples on a filter paper. Afterwards, they were subjected to a stepwise heat treatment at temperatures of 120, 350 and 550 °C for 2 h.

Alkaline synthesis [41] was used to form the catalytic compositions $K_2Ti_2O_5 + K_2Ti_4O_9/TiO_2/TiO_2 + SiO_2$/Ti [34]: the PEO coating doped with TiO_2 nanoparticles ($TiO_2/TiO_2 + SiO_2$/Ti composition), kept for 10 min in a 40% KOH solution. After impregnation, the samples were placed on a filter paper to remove solution excess. Then they were subjected to a subsequent heat treatment in Ar medium for 2 h at a temperature of up to 900 °C. This method allows the synthesis of titanate phases with high speed at relatively low temperatures in an inert atmosphere, without destroying the titanium base.

The excess potassium hydroxide and silicate were removed from the $K_2Ti_2O_5 + K_2Ti_4O_9/TiO_2/TiO_2 + SiO_2$/Ti samples by washing with distilled water until a neutral reaction of the eluate. The samples were then dried in an oven at 150 °C for 1 h and have transferred to a vacuum desiccator, where they were stored at room temperature.

Study of soot combustion

Catalytic combustion of the carbon black was examined on a NETZSCH STA 449 F3 scanning thermogravimetric apparatus in an air flow (50 mL/min) at a heating rate of 5 °C/min on DSC sample carrier with 200 ± 10 mg sample mass. Composites $K_2Ti_2O_5 + K_2Ti_4O_9/TiO_2/TiO_2 + SiO_2$/Ti were coated with soot ("loose" contact) in the burner flame during the combustion of diesel fuel (RF State standard: GOST 305-82) until their mass increased up to 0.15 ± 0.03%. The temperature of the onset of combustion of carbon black (T_o) was determined from the thermogravimetric (TG) curves, the temperature of the maximum combustion rate (T_{max}) was determined from the extremes of the differential calorimetric (DSC) curves, with an accuracy of ± 2 °C.

Surface morphology and composition of samples

The structure of the coatings was investigated using a DRON-7 X-ray diffractometer in Cu K_α radiation. The morphology and elemental composition of the samples were examined by scanning electron microscopy (SEM) (EVO 40 microscope equipped with a Rontec energy dispersive spectrometer, with a refinement of the element content on a 35-SDS JEOL wave dispersion spectrometer). The molar ratio of K:Ti in the potassium titanate phases was calculated on the basis of the element atomic concentrations determined using energy-dispersive analysis.

Evaluation of adhesion and cohesion resistance

The evaluation of the supported layer resistance to adhesive and cohesive failure was carried out by gravimetric method, weighing the samples before and after ultrasonic (US) exposure in an aqueous medium (generator power 100 W, sound frequency 35 kHz), the detailed procedure is reproduced elsewhere [38]. The failure nature of exposed coatings was evaluated by visualization of SEM images. The ultrasonic treatment of prepared samples was carried out under isothermal conditions at 25 °C. The mass of the samples was determined on the NETZSCH STA 449 F3 balance with an accuracy of 10^{-6} g. The initial mass of the coating m_0 was determined from the difference in mass of the coated wire and the same wire mechanically cleaned from the coating to metallic titanium. The mass of the degraded coating Δm was evaluated by weighing the sample before and after the ultrasound exposure, then drying at 150 °C and cooling to room temperature. The duration of individual ultrasound treatments varied from 1 to 20 min, with the total duration of the ultrasound at all the cycles per sample being 30 min.

Evaluation of chemical stability, resistance to heat shock

The chemical stability of potassium titanates in the supported layer to sulfur dioxide (contact time 4 h) and water vapor (1 h) at 400 °C was evaluated by comparing the catalytic properties of the samples before and after inhibiting. Tests on the effect of reaction gases were carried out in a SNOL tube furnace. The total flows of SO_2 and H_2O were 0.14 and 10 g/min, respectively.

The resistance of the samples to heat shock was evaluated on the basis of the decrease in the mass of the samples after one heating–cooling cycle, comparing the catalytic ability of the samples before and after the tests, and changing the morphology of the surface. Heating to a predetermined temperature (800 °C) was carried out in an induction furnace at a rate of 60 °C/min. The creation of a high-temperature gradient was achieved by chilling the samples to 0 °C on a pre-cooled massive metal plate. The cooling rate of the samples was $\sim$ 100–150 °C/s.

Results and discussion

Composition, structure, and catalytic activity of coatings

Fig. 1a shows the SEM image of the anatase particle-modified surface of the PEO coating, after its treatment with KOH solution. There are two main types of sites in the picture. The first is represented by the fine-crystalline phase uniformly

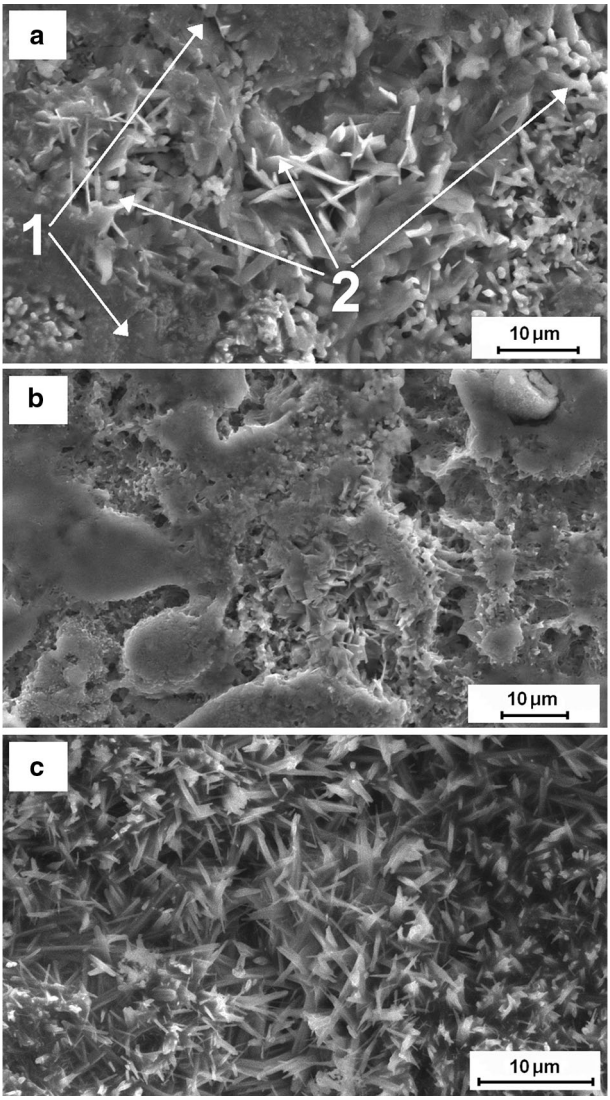

Fig. 1 SEM image of the surface of the $K_2Ti_2O_5 + K_2Ti_4O_9/TiO_2/TiO_2 + SiO_2/Ti$ catalytic composite. **a** Initial coverage (1 and 2 are the main types of sites), **b** US exposed for 30 min in water, **c** after thermal shock

distributed over the surface (1 in Fig. 1a). The second one shows flat crystals of triangular shape up to 5 μm in size and 0.5–1 μm thick (2 in Fig. 1a). According to the energy dispersive analysis, in the first site, the ratio of potassium and titanium ions corresponds to the phase of $K_2Ti_2O_5$, in the second site—$K_2Ti_4O_9$ (Table 1).

It should be noted that the content of silicon is significantly reduced in $K_2Ti_2O_5 + K_2Ti_4O_9/TiO_2/TiO_2 + SiO_2/Ti$ composition with respect to both the initial $TiO_2 + SiO_2/Ti$ and modified anatase nanoparticles of PEO-layers $TiO_2/TiO_2 + SiO_2/Ti$ (Table 1). This may be interpreted by the sample washing after exposure to alkali. Thus, soluble potassium silicates are removed together with the eluate. According to XRD analysis, PEO treatment of titanium leads to the formation of rutile and anatase modification of TiO_2 (Fig. 2a). Moreover, some amount of titanium dioxide is present in the amorphous phase. After deposition of TiO_2 nanoparticles, the fractions of the amorphous phase and anatase increase on the sample surface (Fig. 2b). After alkali impregnation and annealing, $K_2Ti_2O_5$ and $K_2Ti_4O_9$ phases are formed on the surface of $TiO_2/TiO_2 + SiO_2/Ti$ composite (Fig. 2c).

The DSC curve corresponding to the catalytic burning of soot (Fig. 3, curve 1) has one peak of symmetrical shape. So, the process takes place in a single-stage

Table 1 Elemental composition of coatings

Coating	Composite	Elemental composition of outer layer, at.%			
		K	Ti	Si	S
PEO coating	$SiO_2 + TiO_2/Ti$	–	15.4	18.7	–
TiO_2-modified PEO coating	$TiO_2/SiO_2 + TiO_2/Ti$	–	20.3	12.4	–
TiO_2-modified PEO coating impregnated with KOH (1 type site)	$K_2Ti_2O_5/TiO_2/TiO_2 + SiO_2/Ti$	10.6 ÷ 10.7	12.2 ÷ 12.3	3.7 ÷ 3.9	–
TiO_2-modified PEO coating impregnated with KOH (2 type site)	$K_2Ti_4O_9/TiO_2/TiO_2 + SiO_2/Ti$	14.0 ÷ 14.5	27.3 ÷ 27.9	8.3 ÷ 8.8	–
TiO_2-modified PEO coating impregnated with KOH after ultrasonic action for 30 min	$K_2Ti_2O_5 + K_2Ti_4O_9/TiO_2/TiO_2 + SiO_2/Ti$	7.2 ÷ 7.6	18.1 ÷ 18.3	11.4 ÷ 11.8	–
TiO_2-modified PEO coating impregnated with KOH after thermal shock	$K_2Ti_2O_5 + K_2Ti_4O_9/TiO_2/TiO_2 + SiO_2/Ti$	5.9 ÷ 6.1	11.0 ÷ 11.6	7.4 ÷ 7.6	–
TiO_2-modified PEO coating impregnated with KOH after water vapor action	$K_2Ti_2O_5 + K_2Ti_4O_9/TiO_2/TiO_2 + SiO_2/Ti$	8.2 ÷ 8.6	20.5 ÷ 21.5	9.0 ÷ 9.6	–
TiO_2-modified PEO coating impregnated with KOH after sulfur dioxide poisoning	$K_2Ti_2O_5 + K_2Ti_4O_9/TiO_2/TiO_2 + SiO_2/Ti$	6.8 ÷ 7.2	14.1 ÷ 14.7	8.0 ÷ 8.4	0.9–2.1

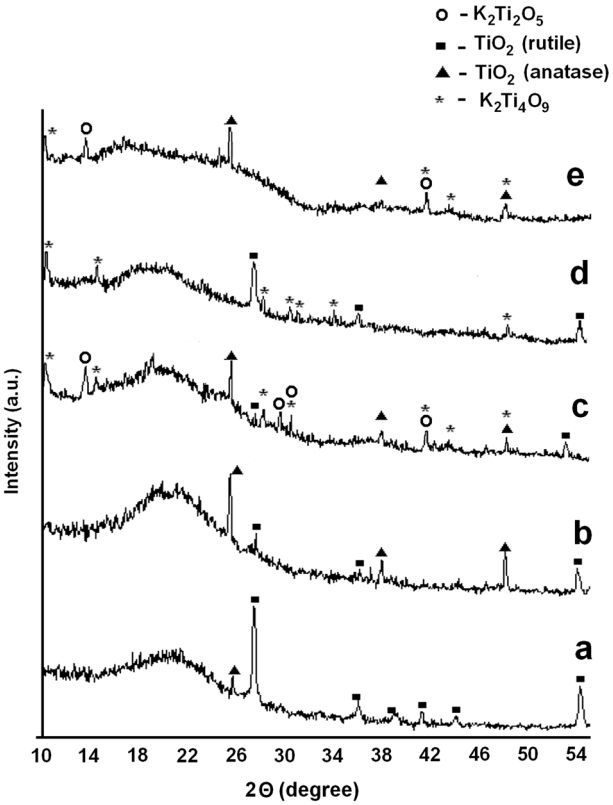

Fig. 2 X-ray diffraction patterns of composites: (a) $TiO_2/SiO_2 + TiO_2/Ti$; (b) $TiO_2/SiO_2 + TiO_2/Ti$; (c) $K_2Ti_2O_5 + K_2Ti_4O_9/TiO_2/TiO_2 + SiO_2/Ti$; (d) $K_2Ti_4O_9/TiO_2/TiO_2 + SiO_2/Ti$ after thermal shock; (e) $K_2Ti_2O_5 + K_2Ti_4O_9/TiO_2/TiO_2 + SiO_2/Ti$ after sulfur dioxide poisoning

mode, the temperature of the beginning of the process is 340 °C, the temperature corresponding to the maximum speed is 390 °C. The results of relatively high catalytic activity for the composition $K_2Ti_2O_5 + K_2Ti_4O_9/TiO_2/TiO_2 + SiO_2/Ti$ are confirmed by literature data for powders of perovskites corresponding to the $xK_2O{\cdot}yTiO_2$ general formula [42].

Evaluation of coating resistance to adhesive and cohesive failure

Under working conditions, the catalytic active part of the coating can be peeled off according to cohesive and adhesive failure due to various mechanical loads (vibration, gas jet impacts, etc.). In this paper, the stability of the obtained composites was evaluated for these types of destruction by the mass decreasing of the sample under the influence of ultrasound [38]. The effect of US on catalytic compositions $K_2Ti_2O_5 + K_2Ti_4O_9/TiO_2/TiO_2 + SiO_2/Ti$ (Table 2) is observed only after 5 min of exposure with mass loss of the sample $\sim$ 0.2% in comparison with the beginning of the test. The maximum loss of coating weight of 0.3% is

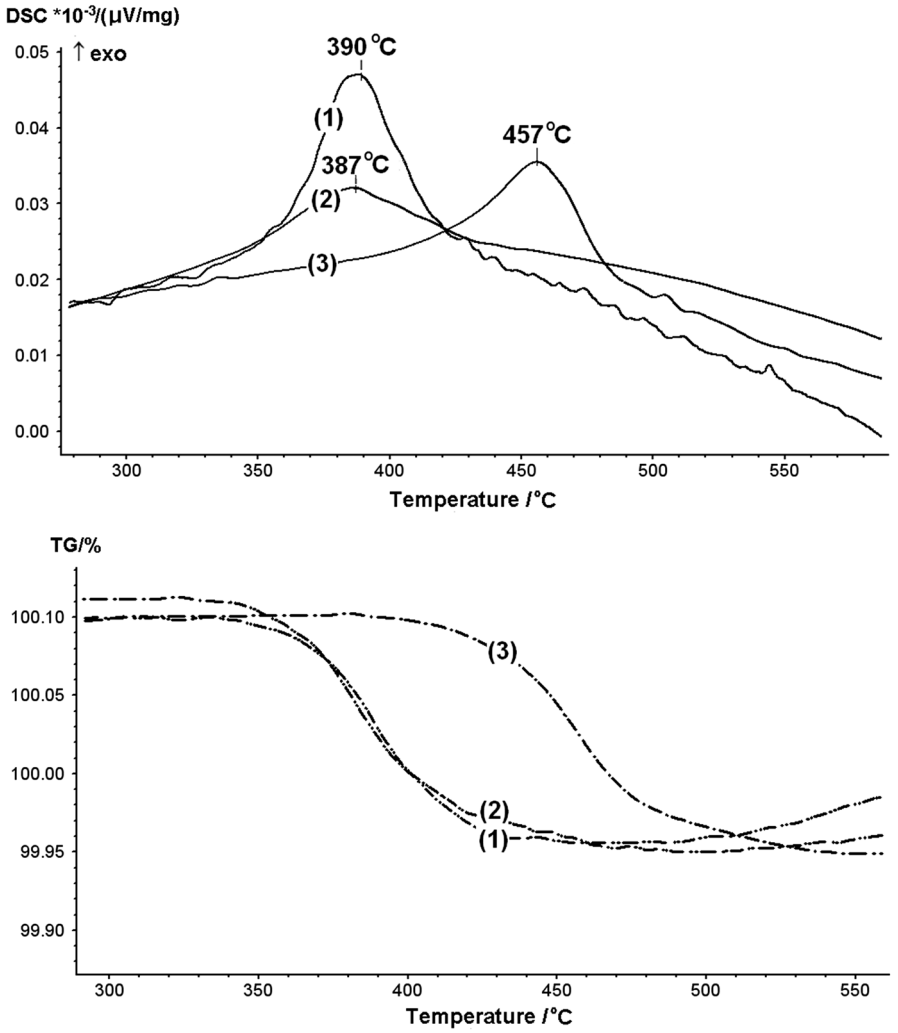

Fig. 3 DSC (solid) and TG (dotted lines) curves of carbon black oxidation in the presence of $K_2Ti_2O_5 + K_2Ti_4O_9/TiO_2/TiO_2 + SiO_2/Ti$ 1—Original compositions; 2—US exposed for 30 min in water; 3—after thermal shock

Table 2 Effect of ultrasonic exposure time on the relative mass loss for the $K_2Ti_2O_5 + K_2Ti_4O_9/TiO_2/TiO_2 + SiO_2/Ti$ composite

τ, min	1	2	3	5	10	30
$\Delta m/m_0 \times 100\%$ (%)	0	0	0	0.2	0.3	0.3

achieved after 10 min of ultrasonic action, with no further reduction in the mass of the sample even after half-hour ultrasonic treatment. Apparently, a slight decrease in the mass of the composite occurs due to the detachment of a part of potassium titanates and unreacted nanoparticles of the anatase sublayer.

The analysis of the SEM images of the initial samples (Fig. 1a) and the samples US-exposed for 30 min (Fig. 1b) revealed no significant changes in the surface morphology of the catalytic layer before and after treatment. The thermal analysis of the soot combustion curves (curves 1 and 2 in Fig. 3) also showed the identity of the catalytic properties of the compared samples. The oxidation of soot in both cases starts from 340 °C and proceeds in a single-stage mode, the values of T_{max} of carbon black combustion and the process termination temperature are comparable too.

Thus, it can be concluded that the catalytic compositions $K_2Ti_2O_5 + K_2Ti_4O_9/TiO_2/TiO_2 + SiO_2/Ti$ have sufficient resistance to adhesive and cohesive failure of catalytically active part of the coating.

Investigation of heat shock resistance

Analysis of the SEM images of $K_2Ti_2O_5 + K_2Ti_4O_9/TiO_2/TiO_2 + SiO_2/Ti$ samples showed that after heating to 800 °C with subsequent abrupt cooling to 0 °C, the coating remains solid without visible fractures and cracks (Fig. 1c). At the same time, the morphology of the surface changes. It is mainly covered with flat crystals of triangular shape up to 5 μm in size and 0.5–1 μm thick corresponded to second type site of initial covering. As it shown in Fig. 2d, all titanium dioxide in the coating is presented in the amorphous phase and rutile modification and there are no XRD reflexes corresponded to $K_2Ti_2O_5$ titanate. So on the surface, $K_2Ti_2O_5$ is replaced by $K_2Ti_4O_9$. This assumption is confirmed by energy-dispersive analysis (Table 1). According to Rudnev et al. [43, 44], up to a temperature of about 700 °C, there is no active penetration of oxygen through the PEO coating to titanium, and no oxidation of the thin metal/coating transition layer is observed. At temperatures above $\sim$ 750 °C, the diffusion of titanium and oxygen along the cracks and pores to the surface (titanium) and into the depth of the coating (oxygen) begins. The surface is enriched in titanium, the oxidation of the latter occurs, up to the formation of rutile crystals. In the case of the investigated coatings in these temperature conditions, the diffusion of potassium ions deep into the oxide-titanium layer also leads to a decrease in the potassium concentration on the surface. The complete replacement of $K_2Ti_2O_5$ by $K_2Ti_4O_9$ in the catalytic layer reduces catalytic activity, which is marked in an increase of the temperature interval for the combustion of carbon black for 70 °C (Fig. 3). This agrees with Wang et al. [42], the authors explain the mechanism of catalytic soot oxidation process in presence of potassium titanates by the formation of surface carbonate intermediates on K^+ ions. So, the decrease in the mole fraction of potassium in a sample of perovskites powders corresponding to the general formula $xK_2O{\cdot}yTiO_2$ leads to an increase of the maximum burning rate temperature.

The thermogravimetric study of the $K_2Ti_2O_5 + K_2Ti_4O_9/TiO_2/TiO_2 + SiO_2/Ti$ catalyst oxidation by the oxygen of the air is shown in Fig. 4. The slow oxidation of

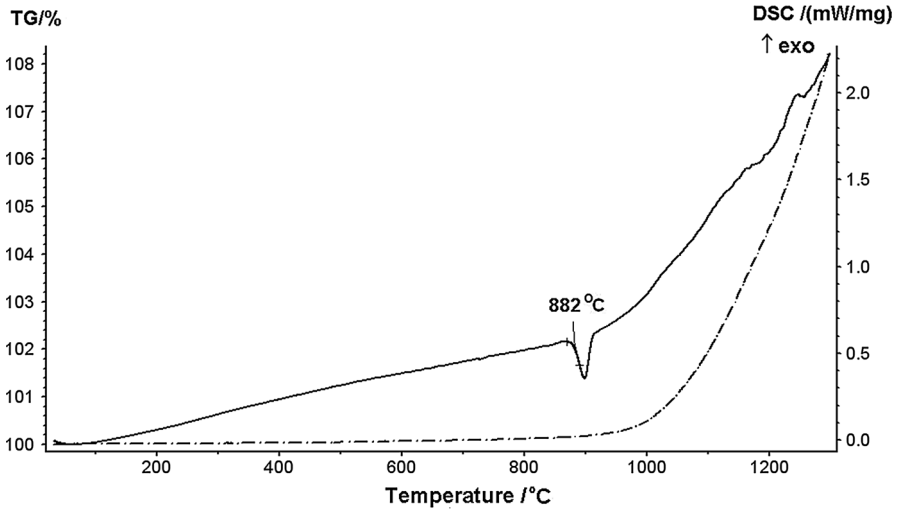

Fig. 4 TG (dotted line) and DSC (solid) curves of the $K_2Ti_2O_5 + K_2Ti_4O_9/TiO_2/TiO_2 + SiO_2/Ti$ catalyst oxidation in the air atmosphere

the titanium base begins at 600 °C. The phase transition of low-temperature α-Ti to high-temperature β-Ti is fixed at 882 °C. Further heating leads to an abrupt increase in the rate of the titanium base oxidation at 900 °C with subsequent catalyst destruction. So, the data obtained in the present paper does not contradict with conclusions reached in [36, 37] on the high-temperature behavior of "PEO-coating/Ti" composites.

Thus, heating to 800 °C followed by an abrupt cooling of the composition $K_2Ti_2O_5 + K_2Ti_4O_9/TiO_2/TiO_2 + SiO_2/Ti$ to 0 °C leads to partial oxidation of the metal base, which is accompanied by a K^+ ion surface concentration decrease and, as a consequence, a decrease in the catalytic activity of the coating. It should also be noted that this exposure does not affect to the continuity of the coating (Fig. 1c).

Influence of inhibitors

Influence of water vapor on the catalyst $K_2Ti_2O_5 + K_2Ti_4O_9/TiO_2/TiO_2 + SiO_2/Ti$ has no significant effect on the oxidation of black carbon. XRD analysis reveals no significant changes in the phase composition of the coating in comparison with the initial one. The maximum temperature value of 389 °C (curve 1 in Fig. 5) is close to the value for the initial catalyst (curve 1 in Fig. 3). A small difference lies within the error of the instrument. The elemental analysis of the surface composition did not reveal a significant reduction of the potassium proportion in the coating composition as compared with the initial (Table 1). This fact explains the permanence of catalytic activity characteristic of coated $K_2Ti_2O_5$ and $K_2Ti_4O_9$ titanates. Thus, noticeable change in the composition, morphology, and catalytic activity is not revealed within prolonged exposure to water vapor on $K_2Ti_2O_5 + K_2Ti_4O_9/TiO_2/TiO_2 + SiO_2/Ti$.

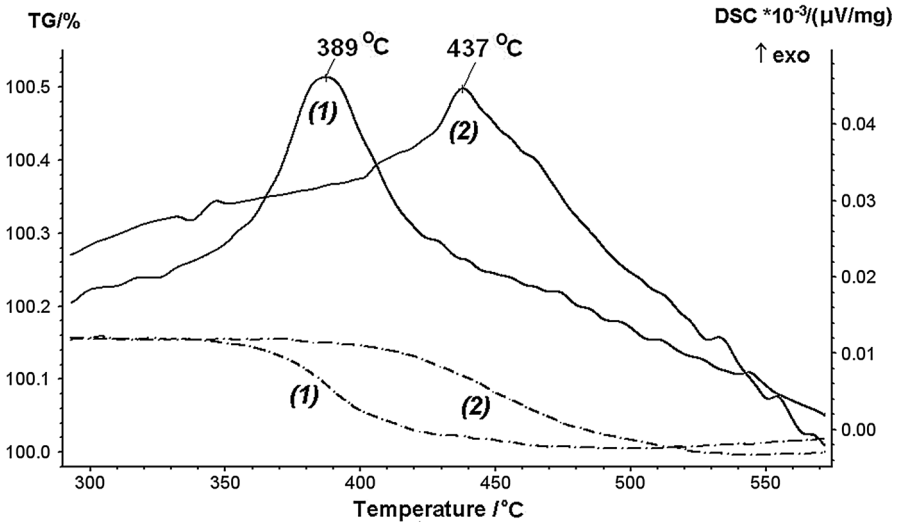

Fig. 5 TG (dotted line) and DSC (solid) curves of carbon black oxidation in the presence of $K_2Ti_2O_5 + K_2Ti_4O_9/TiO_2/TiO_2 + SiO_2/Ti$, subjected to 1—exposure to water vapor; 2—inhibiting effect of sulfur dioxide

The impact of sulfur dioxide on the catalyst compositions leads to a significant increase in the temperature interval of a catalytic combustion of black carbon. The reaction initiation temperature is shifted to 50 °C at higher temperatures (curve 2 in Fig. 5). This indicates a decrease in the catalytic activity of the compositions. It should be noted that the average content of sulfur dioxide in the diesel exhaust is 80 ppm [18] that corresponds to the feed rate of sulfur dioxide 0.076 g/min at the exhaust stream $\sim$ 300 L/min. The flow of SO_2 in our case was 0.14 g/min, the exposure time was 240 min.

Regarding the initial composition, the X-ray diffraction pattern of the $K_2Ti_2O_5 + K_2Ti_4O_9/TiO_2/TiO_2 + SiO_2/Ti$ catalyst after treatment with sulfur dioxide has lower intensities of the reflections of the $K_2Ti_2O_5 + K_2Ti_4O_9$ titanate phases (Fig. 2e). The elemental analysis of the catalyst surface showed the presence of chemisorbed sulfur in an amount of 1–2 at.% (Table 1). Apparently, sulfur dioxide is able to form significantly stronger compounds with potassium than carbon dioxide, so the formation of carbonate intermediates on the surface becomes less possible. However, it should be noted that cerium dioxide CeO_2, commonly used as a carbon black afterburning catalyst, endures a significantly greater reduction in activity when exposed to sulfur dioxide gas at a concentration more than 3 times lower. Namely, the treatment of cerium catalysts with a stream of pure SO_2 for 40 min at a rate of 0.043 g/min leads to the growth of the maximum rate temperature of carbon black catalytic combustion by 111 °C [19].

Thus, it can be concluded that investigated composition exhibits a significantly higher resistance to sulfur dioxide than the currently used cerium dioxide catalysts.

Conclusions

1. $K_2Ti_2O_5 + K_2Ti_4O_9/TiO_2/TiO_2 + SiO_2/Ti$ catalysts were synthesized for the first time using a combination of plasma electrolytic oxidation, deposition of anatase nanoparticles sublayer and alkali method. The process of catalytic burning of soot over these catalysts takes place in a single-stage mode, the temperature of the beginning of the process is 340 °C, and the temperature corresponding to the maximum speed is 390 °C.
2. The surface of catalytic composite contains the sites of two types, which are presented by the fine-crystalline phase uniformly distributed over the surface and the flat crystals of triangular shape up to 5 μm in size and 0.5–1 μm thick. The molar ratio of potassium and titanium ions in these sites corresponds to the phases of $K_2Ti_2O_5$ and $K_2Ti_4O_9$, respectively.
3. It was experimentally established that the catalysts are resistant to ultrasonic treatment, which means a high mechanical resistance and good adhesion of the catalytically active layer to metal substrate.
4. After thermal shock tests, the coatings remain solid, but partially lose their catalytic activity due to the diffusion of titanium onto the surface and replacement of $K_2Ti_2O_5$ by $K_2Ti_4O_9$.
5. The catalysts are resistant to the action of water vapor, but partially poisoned by sulfur dioxide. The poisoning of the $K_2Ti_2O_5 + K_2Ti_4O_9/TiO_2/TiO_2 + SiO_2/Ti$ composite with sulfur dioxide at 400 °C is accompanied by an increase in the temperature of the maximum rate of carbon black catalytic combustion by $\sim$ 50 °C. Such decrease in catalytic activity is caused by chemisorption of SO_2 preventing the formation of carbonaceous intermediates. However, these composites are significantly more resistant to SO_2 than commonly used cerium dioxide catalysts.
6. Thus, the $K_2Ti_2O_5 + K_2Ti_4O_9/TiO_2/TiO_2 + SiO_2/Ti$ composition appears to be a promising catalyst for carbon black afterburning among modern catalysts used in this field.

Acknowledgements The work was partially supported by grants of RFBR No. 18-03-00418 and by the Program "Far East", Project No. 18-3-034.

References

1. Popova NM (1987) Vehicle exhaust catalysts. Nauka, Almaty **(in Russian)**
2. Krylov OV (2004) Heterogeneous catalysis. Akademkniga Publ, Moscow **(in Russian)**
3. van Setten BAAL, Makkee M, Moulijn JA (2001) Science and technology of catalytic diesel particulate filters. Catal Rev Sci Eng 43:489–564
4. Krylova AV, Mikhailichenko AI (2003) Cerium-containing platinum and palladium catalysts. Khim Tekhnol 2:13–21 **(in Russian)**
5. Krishna K, Bueno-López A, Makkee M, Moulijn JA (2007) Potential rare earth modified CeO_2 catalysts for soot oxidation part II: characterisation and catalytic activity with $NO + O_2$. Appl Catal B Environ 75:201–209
6. Guido S, SerraV Badini C, Specchia V (1997) Potential of mixed halides and vanadates as catalysts for soot combustion. Ind Eng Chem Res 36:2051–2058

7. Sui L, Yu LY, Zhang YG (2006) The effects of alkaline earth metals on catalytic activities of K–Sm-based catalysts for diesel soot oxidation. Energy Fuels 20:1392–1397
8. Liu S, Wu X, Weng D, Ran R (2015) Ceria-based catalysts for soot oxidation: a review. J Rare Earth 33:567–590
9. Mukherjee D, Rao BG, Reddy BM (2016) CO and soot oxidation activity of doped ceria: influence of dopants. Appl Catal B Environ 197:105–115
10. Anantharaman AP, Dasari HP, Dasari H, Babu GUB (2018) Surface morphology and phase stability effect of Ceria–Hafnia (CH_x) binary metal oxides on soot oxidation activity. Appl Catal A Gen 566:181–189
11. Mukherjee D, Reddy BM (2018) Noble metal-free CeO_2-based mixed oxides for CO and soot oxidation. Catal Today 309:227–235
12. Wang H, Jin B, Wang H, Ma N, Liu W, Weng D, Wu X, Liu S (2018) Study of Ag promoted Fe_2O_3@CeO_2 as superior soot oxidation catalysts: the role of Fe_2O_3 crystal plane and tandem oxygen delivery. Appl Catal B Environ 237:251–262
13. Andana T, Piumetti M, Bensaid S, Veyre L, Thieuleux C, Russo N, Fino D, Quadrelli EA, Pirone R (2017) Ceria-supported small Pt and Pt_3Sn nanoparticles for NO_x-assisted soot oxidation. Appl Catal B Environ 209:295–310
14. Jin B, Wu X, Weng D, Liu S, Yu T, Zhao Z, Wei Y (2018) Roles of cobalt and cerium species in three-dimensionally ordered macroporous $Co_xCe_{1-x}O_\delta$ catalysts for the catalytic oxidation of diesel soot. J Coll Interface Sci 532:579–587
15. van Doorn J, Varloud J, Moriaudeau P, Perrichon V, Chevrie M, Gauthier C (1992) Effect of support material on the catalytic combustion of diesel soot particulates. Appl Catal B Environ 1:117–127
16. Banus ED, Milt VG, Miro EE, Ulla MA (2010) Co, Ba, K/ZrO_2 coated onto metallic foam (AISI 314) as a structured catalyst for soot combustion: coating preparation and characterization. Appl Catal A Gen 379:95–104
17. Turakulova AO, Zaletova NV, Lunin VV (2010) The dependence of the oxygen-exchange properties of $Ce_{0.5}Zr_{0.5}O_2$ on the method of synthesis. Russ J Phys Chem A 84:1309–1314
18. Gao YX, Wu XD, Liu S, Weng D, Ran R (2016) Effect of water vapor on sulfur poisoning of MnO_x–CeO_2/Al_2O_3 catalyst for diesel soot oxidation. RSC Adv 6:S7033–S7040
19. Flouty R, Abi-Aad E, Siffert S, Aboukaïs A (2003) Role of molybdenum against ceria sulphur poisoning in the combustion of soot particles and the oxidation of propene. Appl Catal B Environ 46:145–153
20. Gross MS, Ulla MA, Querini CA (2009) Catalytic oxidation of diesel soot: new characterization and kinetic evidence related to the reaction mechanism on K/CeO_2 catalyst. Appl Catal A Gen 360:81–88
21. Zhang ZL, Zhang YX, Wang ZP, Gao XY (2010) Catalytic performance and mechanism of potassium-supported Mg–Al hydrotalcite mixed oxides for soot combustion with O_2. J Catal 271:12–21
22. Gong CR, Song CL, Pei YQ, Lv G, Fan GL (2008) Synthesis of $La_{0.9}K_{0.1}CoO_3$ fibers and the catalytic properties for diesel soot removal. Ind Eng Chem Res 47:4374–4378
23. Peng XS, Lin H, ShangguanWF Huang Z (2006) Physicochemical and catalytic properties of $La_{0.8}K_{0.2}Cu_xMn_{1-x}O_3$ for simultaneous removal of NO_x and soot: effect of Cu substitution amount and calcination temperature. Ind Eng Chem Res 45:8822–8828
24. An HM, Kilroy C, McGinn PJ (2004) Combinatorial synthesis and characterization of alkali metal doped oxides for diesel soot combustion. Catal Today 98:423–429
25. Meng XH, Wang Q, Duan LH, Chung JS (2012) Catalytic combustion of diesel soot over perovskite-type catalyst: potassium titanates. Kinet Catal 53:560–564
26. Wang Q, Chung JS, Guo ZH (2011) Promoted soot oxidation by doped $K_2Ti_2O_5$ catalysts and NO oxidation catalysts. Ind Eng Chem Res 50:8384–8388
27. Meng XH, Gao Y, Wang Q, Duan LH (2012) Selective oxidation of PM over Li doped potassium titanate catalysts. China Pet Process Petrochem Techol 14:50–54
28. Meille V (2006) Review on methods to deposit catalysts on structured surfaces. Appl Catal A Gen 315:1–17
29. Ertl G, Knozinger H, Weitkamp J (eds) (1999) Preparation of Solid Catalysts. Wiley-VCH, Verlag **(Federal Republic of Germany)**
30. Gordienko PS, Rudnev VS, Gnedenkov SV, Yarovaya TP, Khrisanfova OA, Tyrin VI, Tyrina LM (1995) Catalytic structures prepared by electrochemical synthesis on metal surfaces. Russ J Appl Chem 68:854–857

31. Tikhov SF, Chernykh GV, Sadykov VA, Salanov AN, Alikina GM, Tsybulya SV, Lysov VF (1999) Honeycomb catalysts for clean-up of diesel exhausts based upon the anodic-spark oxidized aluminum foil. Catal Today 53:639–646
32. Curran J, Clyne T (2006) Porosity in plasma electrolytic oxide coatings. Acta Mater 54:1985–1993
33. Kondrikov NB, Rudnev VS, Vasilyeva MS, Tyrina LM, Yarovaya TP (2005) Prospects for the use in vehicles of oxide film catalysts formed by plasma electrolytic oxidation. Chem Sustain Dev 13:851–853 **(in Russian)**
34. Vasil'eva MS, Rudnev VS, Tyrina LM, Kondrikov NB, Budina AN (2005) Composition and catalytic activity of plasma-electrolytic manganese oxide films on titanium, modified with silver compounds. Russ J Appl Chem 78:1859–1863
35. Vasil'eva MS, Rudnev VS, Kondrikov NB, Tyrina LM, Reshetar AA, Gordienko PS (2004) Catalytic activity of manganese-containing layers formed by anodic-spark deposition. Russ J Appl Chem 77:218–221
36. Lukiyanchuk IV, Rudnev VS, Tyrina LM (2016) Plasma electrolytic oxide layers as promising systems for catalysis. Surf Coat Technol 307:1183–1193
37. Karakurkchi A, Sakhnenko M, Ved M, Galak A, Petrukhin S (2017) Application of oxide-metallic catalysts on valve metals for ecological catalysis. East Eur J Enterp Technol 5:12–18
38. Lebukhova NV, Rudnev VS, Chigrin PG, Lukiyanchuk IV, Pugachevsky MA, Ustinov AYu, Kirichenko EA, Yarovaya TP (2013) The nanostructural catalytic composition $CuMoO_4/TiO_2 + SiO_2$/Ti for combustion of diesel soot. Surf Coat Technol 231:144–148
39. Lebukhova NV, Rudnev VS, Kirichenko EA, Chigrin PG, Lukiyanchuk IV, Karpovich NF, Pugachevsky MA, Kurjavyj VG (2015) The structural catalyst $CuMoO_4/TiO_2/TiO_2 + SiO_2$/Ti for diesel soot combustion. Surf Coat Technol 261:344–349
40. Karpovich NF, Pugachevskij MA, Shtarev DS (2013) The influence of the solvent on the shape of the titanium dioxide crystals during the solvothermal autoclave synthesis. Appl Mech Mater 377:186–190
41. Gorokhovsky AV (2008) Method for the preparation of potassium titanate. Patent RF 2326051 C1. Bull vol. 16
42. Wang Q, Guo ZH, Chung JS (2009) Formation and structural characterization of potassium titanates and the potassium ion exchange property. Mater Res Bull 44:1973–1977
43. Rudnev VS, Malyshev IV, Lukiyanchuk IV, Kuryavyi VG (2012) Composition, surface structure, and thermal behavior of $ZrO_2 + TiO_2$/Ti and $ZrO_2 + CeO_x + TiO_2$ composites formed by plasma-electrolytic oxidation. Prot Met Phys Chem Surf 48:455–461
44. Vasilyeva MS, Rudnev VS, Wiedenmann F, Wybornov S, Yarovaya TP, Jiang X (2011) Thermal behavior and catalytic activity in naphthalene destruction of Ce-, Zr- and Mn-containing oxide layers on titanium. Appl Surf Sci 258:719–726